

1-Methyl-4-[2-(3-methoxy-4-hydroxyphenyl)ethenyl]pyridinium] hydrogensquarate monohydrate: synthesis, structural investigations and optical properties

B. B. Koleva · T. Kolev · M. Spitteller ·
H. Mayer-Figge · W. S. Sheldrick

Received: 3 November 2008 / Accepted: 6 February 2009 / Published online: 24 February 2009
© Springer Science+Business Media B.V. 2009

Abstract 1-methyl-4-[2-(3-methoxy-4-hydroxyphenyl)ethenyl]pyridinium] hydrogensquarate monohydrate (**1**) has been synthesized and its structure obtained by single crystal X-ray diffraction. Optical properties have been elucidated by means of linear-polarized solid state IR-spectroscopy, UV-spectroscopy as well as nuclear magnetic resonance and thermal analysis. The polarization tool of oriented colloid suspensions in nematic host is used. Quantum chemical calculations have performed with a view to obtaining the electronic structure and optical properties of the novel compound. The compound crystallizes in the space group P-1 and the structure consists of infinite layers, resulting from intermolecular OH...O=C_(sq) (2.684 Å) and _(sq)OH...OH₂ (2.575 and 2.850 Å) hydrogen bonds between the cation and anions as well as solvent molecules.

Keywords

1-methyl-4-[2-(3-methoxy-4-hydroxyphenyl)ethenyl]pyridinium] hydrogensquarate monohydrate · Single crystal X-ray data · Solid-state linear polarized IR-spectroscopy · NLO application · UV-Vis · MS · TGV and DSC

Introduction

As a part of our systematic investigations of stybazolium salts and their derivatives, possessing large second order molecular hyperpolarizabilities [1–4], we now present a spectroscopic and structural elucidation of 1-methyl-4-[2-(3-methoxy-4-hydroxyphenyl)ethenyl]pyridinium] hydrogensquarate monohydrate (**1**) (Scheme 1) [5–9]. Obtained, nonlinear optical manifestation of the alignment of thin films of the quinoide form of 1-methyl-4-[2-(3-methoxy-4-oxocyclohexadienylidene)ethylidene]-1,4-dihydropyridin, deposited on mica (Fig. 1) [10], provoke us for systematic study of the relationship structure-spectroscopic properties of the entitled compound.

Methods, such as single crystal X-ray diffraction, UV-Vis spectroscopy, polarized linear dichroic infrared (IR-LD) spectroscopy of oriented colloid suspensions in a nematic liquid crystal, mass spectrometry, TGV and DSC methods. Quantum chemical calculations have performed with a view to obtaining the electronic structure and optical properties of the cationic 1-methyl-4-[2-(3-methoxy-4-hydroxyphenyl)ethenyl]pyridine.

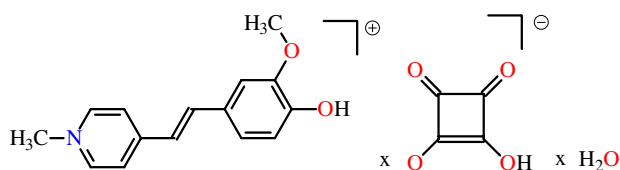
Experimental

Materials and methods

The X-ray diffraction intensities were measured in the ω scan mode on a Siemens P4 diffractometer equipped with Mo K $_{\alpha}$ radiation ($\lambda = 0.71073 \text{ \AA}$, $\theta_{\max} = 25^{\circ}$) and the structure was solved by direct methods and refined against F_o^2 [11, 12]. An ORTEP plot illustrates the anion and cation structures at the 50% probability level. Relevant crystallographic structure data and refinement details are

B. B. Koleva (✉) · H. Mayer-Figge · W. S. Sheldrick
Lehrstuhl für Analytische Chemie, Ruhr-Universität Bochum,
Universitätsstraße 150, 44780 Bochum, Germany
e-mail: BKoleva@chem.uni-sofia.bg

T. Kolev · M. Spitteller
Institut für Umweltforschung, Universität Dortmund,
Otto-Hahn-Strasse 6, 44221 Dortmund, Germany



Scheme 1 Chemical diagram of titled compound (1)

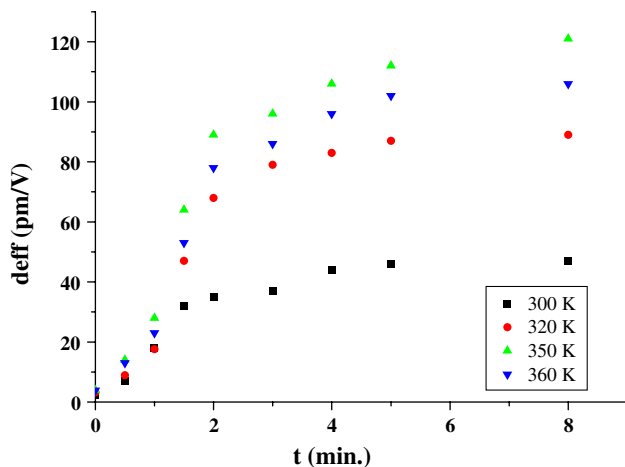


Fig. 1 Dependence of the second-order susceptibilities at 1,064 nm versus the time with frequency repetition about 1 kHz [10]

presented in Table 1, selected bond distances and angles in Table 2. The hydrogen atoms were constrained to calculated positions and refined using riding models in all cases. The obtained disorder in the hydrogensquarate fragment in

the crystal is on the base of the obtained relatively higher R-factor of the final refinement. This phenomenon has been previously reported and observed for these dyes [9].

The IR-spectra were measured on a Thermo Nicolet OMNIC FTIR-spectrometer (4,000–400 cm^{-1} , 2 cm^{-1} resolution, 200 scans) equipped with a Specac wire-grid polarizer. Non-polarized solid-state IR spectra were recorded using the KBr disk technique. The oriented samples were obtained as a suspension in a nematic liquid crystal (MLC 6815, Merck) with the presence of an isolated nitrile stretching IR-band at about 2,245 cm^{-1} additionally serving as an orientation indicator. The theoretical approach and the, experimental technique for preparing the samples, procedures for polarized IR-spectra interpretation and the validation of this new linear-dichroic infrared (IR-LD) orientation solid-state method for accuracy, precision and the influence of the liquid crystal medium on peak positions and integral absorbances of the guest molecule bands have been presented previously [13–16]. The nature and balance of the forces in the nematic liquid crystal suspension system, the mathematical model for their clearance, the morphology of the suspended particles and the influence of the space group types on the degree of orientation (*i.e.* the ordering parameter) have been investigated [16] using five liquid crystals and fifteen compounds. The applicability of the last approach to experimental IR-spectroscopic band assignment as well as in obtaining stereo-structural information has been demonstrated in a series of organic systems and coordination complexes of heterocyclic ligands, Cu(II)

Table 1 Crystal data, intensity collection and refinement conditions for (1)

Empirical formula	$\text{C}_{19}\text{H}_{18}\text{NO}_6$	
Formula weight	356.34	
Temperature	293(2) K	
Wavelength	0.71073 Å	
Crystal system, space group	Triclinic, P-1	
Unit cell dimensions	$a = 8.151(3)$ Å	$\alpha = 76.497(10)^\circ$
	$b = 9.3411(15)$ Å	$\beta = 83.77(2)^\circ$
	$c = 12.6226(16)$ Å	$\gamma = 88.17(2)^\circ$
Volume	928.969 Å ³	
Z	2	
Calculated density	1.274 Mg/m^3	
Absorption coefficient	0.096 mm^{-1}	
$F(000)$	374	
Crystal size	0.44 × 0.50 × 0.40 mm	
θ Range for data collection	2.47 to 25.00°	
Limiting indices	$-1 \leq h \leq 9, -10 \leq k \leq 10, -15 \leq l \leq 15$	
Reflections collected/unique	3892/3180 [$R(\text{int}) = 0.0448$]	
Refinement method	Full-matrix least-squares on F^2	
Goodness-of-fit on F^2	1.040	
Final R indices [$I > 2\sigma(I)$]	$R1 = 0.0676, wR2 = 0.1639$	
R indices (all data)	$R1 = 0.1462, wR2 = 0.2043$	

Table 2 Selected bond lengths [Å] and angles [°] for (1)

O29 C40 1.249(4)	C9 C11 1.455(5)	O33 C49 1.423(5)
C40 C47 1.454(5)	C10 C20 1.383(5)	O51 C51 1.291(13)
O2 C7 1.361(4)	C11 C35 1.327(5)	C51 C50 1.474(12)
C5 C31 1.391(5)	N12 C25 1.333(5)	C51 C52 1.472(14)
C5 C34 1.393(5)	N12 C42 1.339(5)	O50 C50 1.206(9)
C5 C35 1.465(5)	N12 C37 1.489(4)	O53 C53 1.221(9)
C7 C20 1.367(5)	C21 C26 1.372(5)	C50 C53 1.491(11)
C7 C26 1.402(5)	C25 C34 1.360(5)	C53 C52 1.482(13)
C9 C21 1.392(5)	C26 O33 1.366(4)	O52 C52 1.234(13)
C9 C10 1.401(5)	C31 C42 1.356(5)	
O29 C40 C47 135.7(4)	C10 C9 C11 122.8(4)	O33 C26 C21 125.0(3)
C31 C5 C34 116.8(3)	C20 C10 C9 120.1(4)	O33 C26 C7 115.0(3)
C31 C5 C35 119.9(3)	C35 C11 C9 126.9(4)	C21 C26 C7 119.9(4)
C34 C5 C35 123.3(4)	C25 N12 C42 120.0(3)	C42 C31 C5 120.8(4)
O2 C7 C20 122.6(3)	C25 N12 C37 120.3(3)	C26 O33 C49 117.0(3)
O2 C7 C26 118.3(3)	C42 N12 C37 119.6(4)	C25 C34 C5 120.0(4)
C20 C7 C26 119.1(3)	C7 C20 C10 121.4(4)	C11 C35 C5 125.7(4)
C21 C9 C10 118.0(3)	C26 C21 C9 121.5(3)	N12 C42 C31 120.8(4)
C21 C9 C11 119.2(3)	N12 C25 C34 121.5(4)	

complexes, polymorphs, codeine derivatives, Au(III) peptide complexes and their hydrochlorides and hydrogensquarates [16–20]. The theory of IR-LD spectroscopy and the employed polarized IR-spectra interpretation difference-reduction procedure are given in references [21–24].

Ultraviolet (UV-) spectra were recorded on Tecan Safire Absorbance/Fluorescence XFluor 4 V 4.40 spectrophotometer operating between 190 and 900 nm, using the solvents water, methanol, dichloromethane, tetrahydrofuran, acetonitrile, acetone, 2-propanol and ethyl acetal (all Uvasol, Merck products) at concentrations of 2.5×10^{-5} M, using 0.0921 cm quartz cells.

Quantum chemical calculations are performed with GAUSSIAN 98 and Dalton 2.0 program packages [25, 26]. The output files are visualized by means of the ChemCraft program [27]. Geometry was optimized at two levels of theory: restricted Hartree-Fock (RHF) and density functional theory (DFT) using 6-31 ++G** basis set. In second case, the B3LYP method, which combines Becke's three-parameter non-local exchange functional with the correlation function of Lee, Yang and Parr is applied. Molecular geometries of the studied species were fully optimized by the force gradient method using Bernys' algorithm. For every structure, the stationary points found on the molecule potential energy hyper surfaces were characterized using standard analytical harmonic vibrational analysis. Absence of the imaginary frequencies and negative eigenvalues of the second-derivative matrix confirmed that the stationary points correspond to minima of the potential energy hyper surfaces. The calculation of vibrational frequencies and infrared intensities were checked for which kind of calculations performed agree best with the experimental data. In

our case the DFT method provide more accurate vibrational data, as far as the calculated standard deviations are about 5 cm^{-1} (B3LYP) and 9 cm^{-1} (HF), respectively. B3LYP/6-31G* data are presented for above discussed modes, where for the better correspondence between the experimental and theoretical values, a modification of the results using the empirical scaling factor 0.9614 was made. In the case of HF calculations, the scaling factor of 0.8929 was used. The solvent effect on the absorption bands were studied by TD [27] DFT level of theory with a combination of polarized continuum model (PCM) [28–30].

Synthesis

The starting compounds for the synthesis of (1), 1,4-dimethylpyridinium iodide and 3-methoxy-4-hydroxybenzaldehyde were Merck (Germany) products. The reaction scheme for obtaining of 1-methyl-4-[2-(3-methoxy-4-hydroxyphenyl)ethenyl]pyridinium iodide is: 2.3500 g (10.0 mmol) 1,4-dimethylpyridinium iodide is mixed with 1.2200 g (10.0 mmol) 3-methoxy-4-hydroxybenzaldehyde in 50.0 ml toluene. 5.00 ml acetic acid and 0.77 g (10.00 mmol) ammonium acetate are also added to the reaction mixture. The resulting suspension is stirring for 24 h at room temperature. Then 0.50 ml concentrated HI and 10.00 ml ethanol are added and the obtained reaction mixture left to stand for 16 h at room temperature. The resulting orange precipitate is filtered off, washed with $\text{C}_2\text{H}_5\text{OH}$ and dried on P_2O_5 at 298 K. 1-methyl-4-[2-(3-methoxy-4-oxocyclohexadienylidene)ethylidene]-1,4-dihydropyridine is then obtained in the following way: 10.0 mg of iodide salt are dissolved in 10.00 mmol ethanol and then 5 ml 1.0 M KOH

are added. The obtained lila solution is heated for 2 h at a temperature of 70°C, and then is kept at 4°C for 16 h. The resulting violet precipitate is filtered off and, dried on P₂O₅ at 298 K. Finally, (1) is obtained by mixing equimolar amounts of the quinolid derivative and squaric acid in 20 ml ethanol. The obtained mixture is stirred for 2 h at 40°C. The obtained solution is cooled to 4°C and held at this temperature for 10 h. Finally the resulting orange crystals are filtered off, washed with methanol and dried on P₂O₅ at 298 K. Yield 42%.

Results and discussion

Crystal structure and molecular geometry

The compound (1) crystallizes in the centrosymmetric space group P-1 (Fig. 2). Similar to 1-methyl-4-[2-(4-hydroxyphenyl)ethenyl]pyridinium] hydrogenphosphate [9], infinite layers are formed by intermolecular hydrogen bonds of the types OH...O=C_(sq) (2.684 Å) and _(sq)OH...OH₂ (2.575 and 2.850 Å) (Fig. 3). The interlayers interaction is in the basis of the obtained optical properties of this compound. One of the hydrogensquarate anions is disordered, which is typical for systems containing this counterion (Fig. 3). The geometry of the cation is effectively flat with a maximal deviation of 0.5(8)°. The OCH₃ group lies in the plane of 1-methyl-4-[2-(4-hydroxyphenyl)ethenyl]pyridinium] fragment with an angle (H₃)COCC(H) of 4.7(1)° with Z 2, the unit cell contains two co-planar disposed cations at a distance of 3.460 Å, thus causing a co-linear orientation of the out-of-plane (o.p.) B₁ transition moments of the aromatic fragments.

The most stable conformer of the 1-methyl-4-[2-(3-methoxy-4-hydroxyphenyl)ethenyl]pyridinium] cation is characterized with the E value of 0.2 kJ/mol. The optimized geometry parameters are depicted in Scheme 2. The conformer with the opposite orientation of the OH-group is characterized with the higher energy of 3.2 kJ/mol, due to

Fig. 2 The molecular structure of (1). Displacement ellipsoids are drawn at the 50% probability level

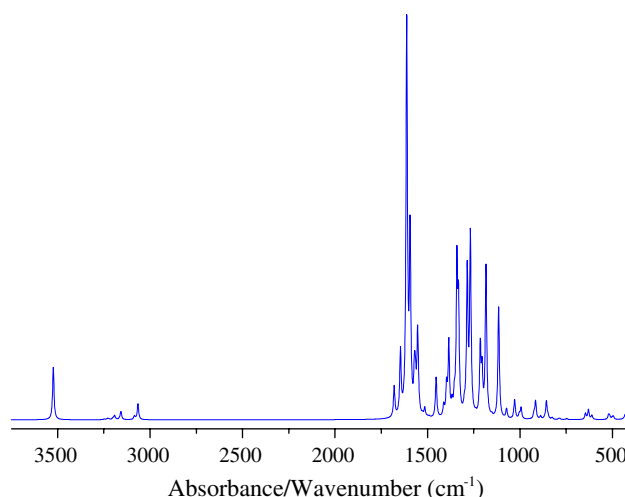
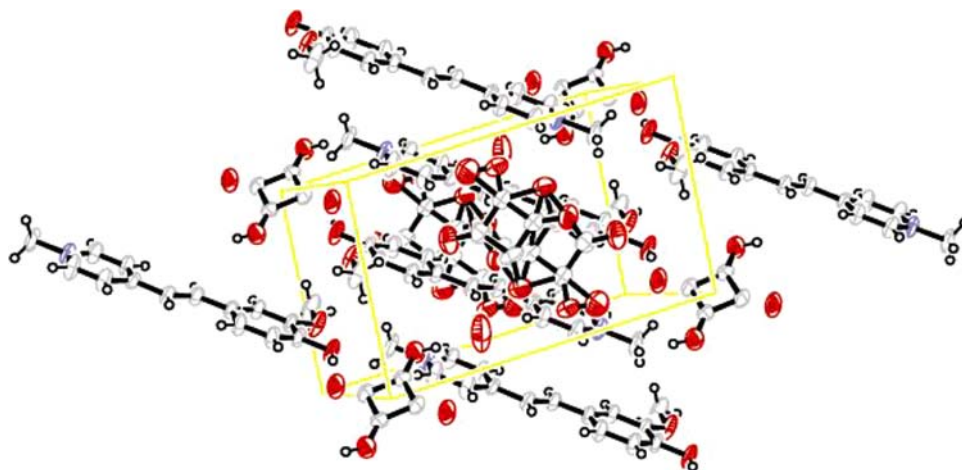


Fig. 3 Theoretical IR-spectrum of 1-methyl-4-[2-(3-methoxy-4-hydroxyphenyl)ethenyl]pyridinium] cation

the underlined steric effect with the OCH₃-substituent at 3-position. The molecule is effectively flat with a deviation of 0.1(7)°. A good correlation between the theoretically predicted values for the geometry and experimental values obtained by single crystal X-ray diffraction was obtained (Compare Scheme 2 and Table 2). The values differ by less than 0.025 Å and 2.2(1)°. The molecule is flat with a deviation of 1.6(3)°. The 3-substituent lies in the plane of the molecule with an angle of 0.2(1)°, respectively.

Vibrational properties and polarized IR-spectroscopic data

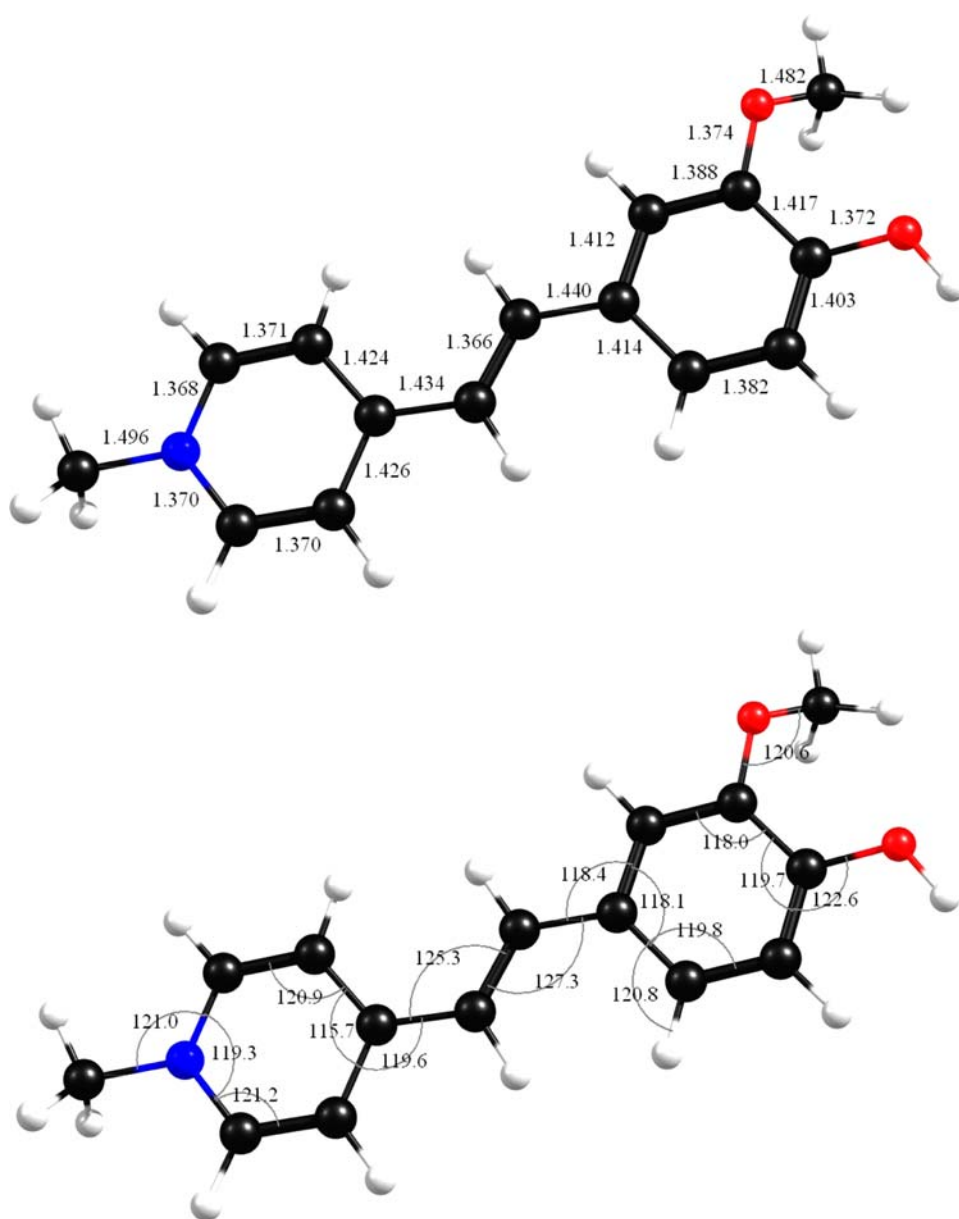
The observed significant degree of macro-orientation in the polarized IR-spectrum of sample facilitates an adequate interpretation of the polarized IR-data and results from the presence of a pseudo layer structure, which adopts a macro-orientation in the solid phase toward the orientation director (**n**) of the liquid crystal. The detailed IR-LD

spectroscopic analysis is supported by the theoretical vibrational analysis at the B3LYP/6-31++G** level. The calculated IR-spectrum is depicted in Fig. 3.

The highest frequency band at $3,523\text{ cm}^{-1}$ corresponds to the ν_{OH} stretching vibration. In the solid state (see below) the corresponding IR-maximum is shifted to lower frequency more than 200 cm^{-1} as a result of the participation of the OH-group in intermolecular hydrogen bonding. The bands within the $3,000\text{--}3,100\text{ cm}^{-1}$ and $1,640\text{--}1,450\text{ cm}^{-1}$ range belong to in-plane (i.p.) A_1 and/or B_2 stretching vibrations of the aromatic rings and as a rule the pyridinium ones are higher frequency observed. The o.p. B_1 bands are observed within the $900\text{--}680\text{ cm}^{-1}$ range and the corresponding transition moments are perpendicularly oriented to the plane of the cation (Scheme 3).

The non-polarized IR-spectrum shows a relatively intensive band at $3,300\text{ cm}^{-1}$ corresponding to the stretching ν_{OH} vibration of the hydrogen bonded OH-group in merocyanine dyes, thus correlating with the obtained crystallographic data. The broad absorption band between $3,000$ and $1,900\text{ cm}^{-1}$ is attributed to ν_{OH} of dihydrogensquarate anions (HSq^-). Bands at $1,795\text{ cm}^{-1}$, $1,685\text{ cm}^{-1}$ and $1,589\text{ cm}^{-1}$ correspond to $\nu_{\text{C}=\text{O}}$, $\nu_{\text{C}=\text{O}}^{\text{as}}$ and $\nu_{\text{C}=\text{C}}$ vibrations of the HSq^- anions (Fig. 4). Aromatic in-plane modes of the benzene and pyridine rings are at $1,620\text{ cm}^{-1}$ ($\mathbf{8a}_{(\text{py})}$) and $1,600\text{ cm}^{-1}$ ($\mathbf{8a}_{(\text{Ph})}$), respectively. The theoretical values are $1,618\text{ cm}^{-1}$ and $1,598\text{ cm}^{-1}$, respectively. The band at $1,338\text{ cm}^{-1}$ corresponds to the symmetric bonding vibration of the N-CH_3 group ($\delta_{\text{CH}_3}^{\text{s}}$) and the obtained value is similar to those of other

Scheme 2 Geometrical parameters of the most stable conformer of 1-methyl-4-[2-(3-methoxy-4-hydroxyphenyl)ethenyl]pyridinium] cation



Scheme 3 Visualization of the selected B_1 transition moments in the 1-methyl-4-[2-(3-methoxy-4-hydroxyphenyl) ethenyl]pyridinium] cation

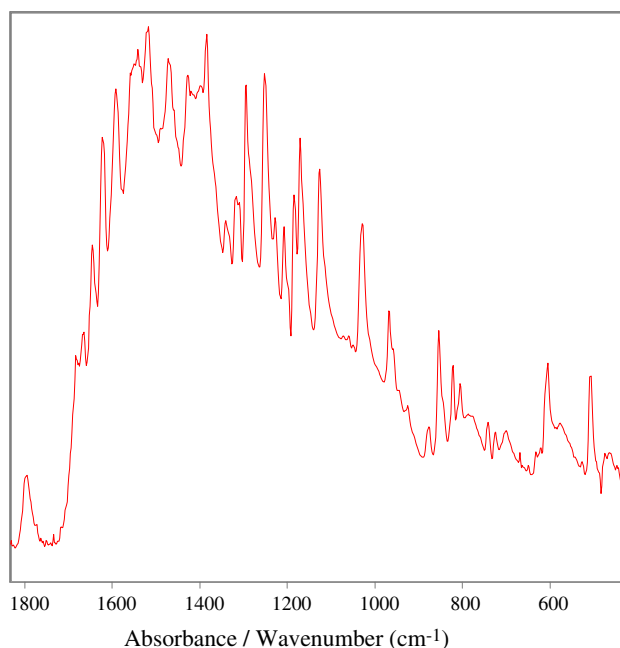
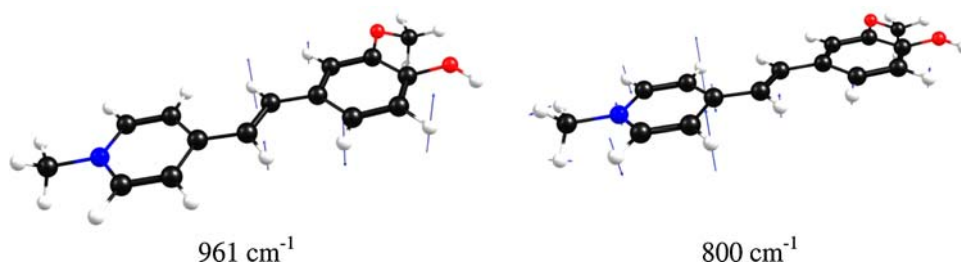


Fig. 4 Non-polarized IR-spectrum of (1) within the range 1,810–400 cm^{-1}

merocyanine dyes studied with a difference of less than $\pm 3 \text{ cm}^{-1}$ [9]. The absorption maxima belonging to the out-of-plane bending vibrations $\gamma_{\text{C}=\text{C}}$, $11-\gamma_{\text{CH}}$ benzene and of the pyridine rings are observed at 960 cm^{-1} (calc. 961 cm^{-1}), 856 cm^{-1} (calc. 855 cm^{-1}) and 805 cm^{-1} (calc. 800 cm^{-1}). Spectroscopic support for the X-ray structure is obtained by application of the reducing difference procedure to polarized IR-spectra, where the elimination of the last bands at equal dichroic ratio is obtained (Fig. 5), due to the corresponding transition moments being oriented in a co-linear manner (see Scheme 3). This result indicates the co-planar disposition of aromatic rings and double bonds (Fig. 2, Scheme 2) and is in good agreement with the crystallographic structure.

Electronic spectra

The possible redistribution of the electronic density in these compounds as typical push-pull systems depends of the solvent polarity. When the electron transition is connected with intramolecular charge transfer (CT), this leads

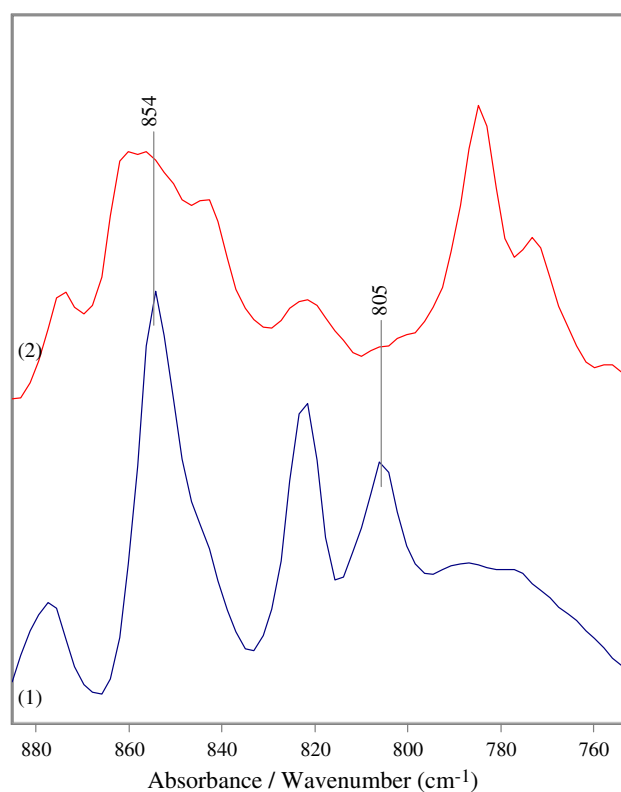


Fig. 5 Non-polarized IR-(1) and reduced IR-LD (2) spectrum of (1) after the elimination of the band at 805 cm^{-1}

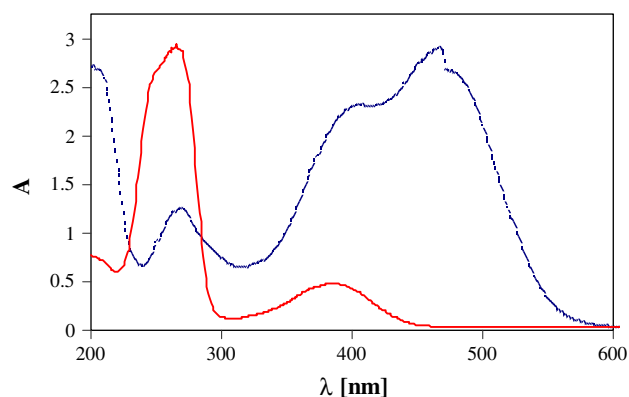


Fig. 6 UV-Vis spectra of (1) and the quinoid form of the dye (dotted line) in aqueous solution at a concentration of $2.5 \cdot 10^{-5} \text{ M}$

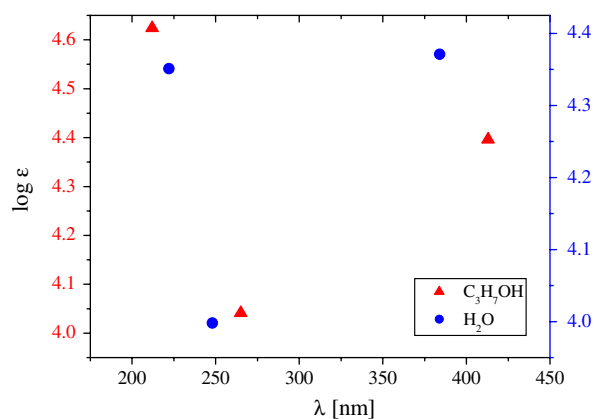
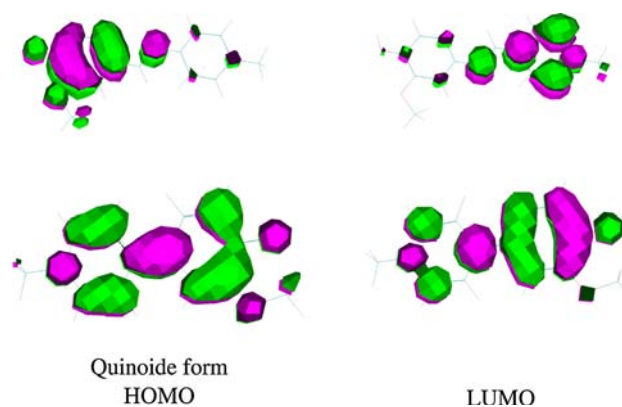


Fig. 7 The dependence λ [nm] and $\log \epsilon$ for the solvents 1-propanol and water of 1-methyl-4-[2-(3-methoxy-4-hydroxyphenyl)ethenyl]pyridinium] hydrogensquarate monohydrate

to a significant difference between the dipole moment in the ground and excited states, that determines their significant solvatochromism, or NLO properties in solution (Figs. 6, 7). Depending on the solvent polarity, the CT band in 1-methyl-4-[2-(3-methoxy-4-hydroxyphenyl)ethenyl]pyridinium] hydrogensquarate monohydrate exhibits



Scheme 4 Molecular orbital surface of the HOMO and LUMO for the ground state of the cation and its quinoid form

a bathochromic shift of up to 70 nm on going from H_2O to 1,2-dichloromethane. The observed negative solvatochromic effect in these compounds has been explained by both intra and intermolecular charge transfer.

The distribution of the highest occupied (HOMO) and lowest unoccupied (LUMO) molecular orbitals for the ground state is illustrated in Scheme 4. Nearly all of the

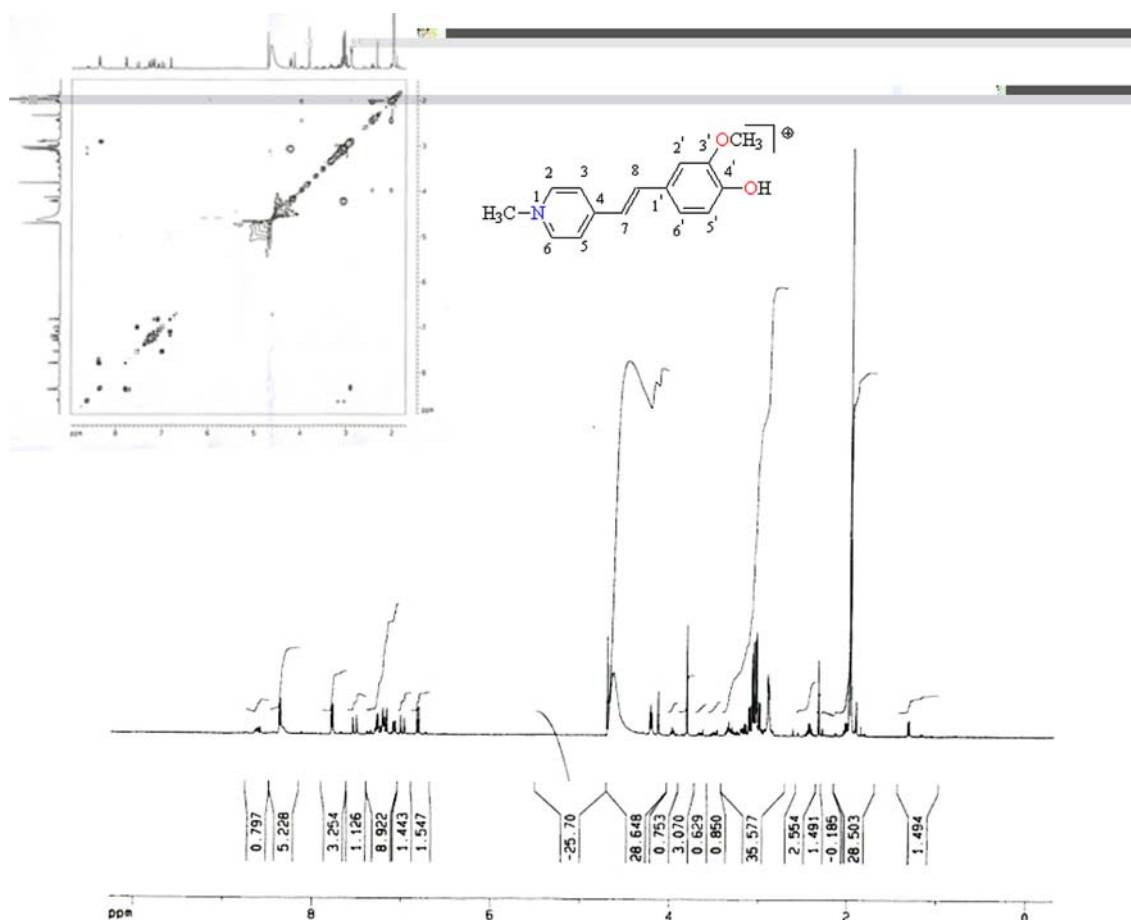


Fig. 8 ^1H - and $^1\text{H},^1\text{H}$ -COSY NMR spectra of compound studied in D_2O solution

MOs are substantially localized in the conjugated plane in the quinoid form, with only small contributions to the group out of the plane. These data are similar to previously reported ones of the other dyes [31]. However, the MOs are localized on both aromatic fragments (Scheme 4).

For a precise investigation of the geometry changes associated with the electronic excitation, to the lowest singlet excited state, the geometry of the compounds was optimized at the CIS/6-31 ++G** level of theory for the comparison with the data for the ground state optimized at HF/6-31 ++G**. A similar approach has been previously used [32]. The data indicate that the structural shift is predominantly localized in the conjugated plane and that the groups out of the discussed plane are not significantly changed. The distribution for the HOMO and LUMO for the lowest single excited state shows a strongest optical emission.

¹H-NMR data

The ¹H and ¹H,¹H-COSY NMR spectra of (**1**) are depicted in Fig. 8. The assignment of the chemical shift signals is carried out using the numbering scheme in same figure. The data are follows: 3.88 (s, 3H, OCH₃), 4.72 (s, 3H, N-CH₃), 6.81 (d, 1H, H-5'), 7.18 (dd, 1H, H-6'), 7.30 (d, 1H, H-2'), 7.38 (1H, H-8), 7.91 (1H, H-7), 8.14 (2H, H-2, H-6), 8.76 (2H, H-3, H-5) and 9.77 ppm (s, 1H, OH).

Supporting information

Crystallographic data for the structural analysis have been deposited with the Cambridge Crystallographic Data Centre, CCDC 697436 Copies of this information may be obtained from the Director, CCDC, 12 Union Road, Cambridge, CB2 1EZ, UK (Fax: +44 1223 336 033; e-mail: deposit@ccdc.cam.ac.uk or <http://www.ccdc.cam.ac.uk>).

Acknowledgements B.K. wishes to thank the Alexander von Humboldt Foundation for the Fellowship and T.K. the DAAD for a grant within the priority program “Stability Pact South-Eastern Europe” and the Alexander von Humboldt Foundation.

References

- Marder, S.R., Perry, J.W., Schaefer, W.P.: Synthesis of organic salts with large second-order optical nonlinearities. *Science* **245**, 626–628 (1989)
- Marder, S.R., Perry, J., Tiemann, S., Warsh, T., Schaefer, W.: Second-order optical nonlinearities and photostabilities of 2-N-methylstilbazolium salts. *Chem Mater.* **2**, 685–690 (1990)
- Ashwell, G.J., Hargreaves, R.C., Baldwin, C., Bahra, G., Brown, C.R.: Strong second-harmonic generation from centrosymmetric dyes. *Nature* **375**, 385–388 (1992)
- Lupo, D., Prass, W., Scheunemann, U., Laschewsky, A., Ringsdorf, R., Ledoux, I.: Second-harmonic generation in Langmuir-Blodgett monolayers of stilbazium salt and phenylhydrazone dyes. *J. Opt. Soc. Am. B* **5**, 300–307 (1988)
- Kolev, T.M., Yancheva, D.Y., Stoyanov, S.I.: Synthesis, spectral and structural elucidation of some pyridinium betaines of squaric acid—potential materials for nonlinear optical applications. *Adv. Func. Mater.* **14**, 799–804 (2004)
- Kolev, T., Wortmann, R., Spitteller, M., Sheldrick, W.S., Heller, M.: 4-Methoxypyridinium betaine of squaric acid. *Acta Crystallogr.* **E60**, o1374–o1376 (2004)
- Kolev, T., Wortmann, R., Spitteller, M., Sheldrick, W., Mayer-Figge, H.: 4-Phenylpyridinium betaine of squaric acid. *Acta Crystallogr.* **E61**, o1090–o1093 (2005)
- Kolev, T., Stamboliyska, B., Yancheva, D.: Spectral and structural study of two acceptor-substituted pyridinium-betaines of squaric acid: promising chromophores for nonlinear optical applications. *Chem. Phys.* **324**, 489–496 (2006)
- Kolev, T., Koleva, B., Spitteller, M., Mayer-Figge, H., Sheldrick, W.S.: Synthesis, spectroscopic and structural characterization of 1-methyl-4-[2-(4-hydroxyphenyl)ethenyl]pyridinium dihydrogenphosphate. *Dyes Pigm.* **79**(1), 7–13 (2008)
- Kolev, T., Koleva, B., Tkaczyk, S., Kityk, I., Spitteller, M., Perona, A.: Nonlinear optical manifestation of alignment of thin films of dihydropyridin organic chromophore deposited on mica substrate. *J. Mater. Sci.* (2009). doi:10.1007/s10854-008-9828-5
- Sheldrick, G.M.: SHELXTL, Release 5.03 for Siemens R3 crystallographic research system. Siemens Analytical X-Ray Instruments, Inc, Madison, USA (1995)
- Sheldrick, G.M.: SHELXS97 and SHELXL97. University of Goettingen, Germany (1997)
- Ivanova, B.B., Arnaudov, M.G., Bontchev, P.R.: Linear-dichroic infrared spectral analysis of Cu(I)-homocysteine complex. *Spectrochim. Acta* **60**(4A), 855–862 (2004)
- Ivanova, B.B., Tsalev, D.L., Arnaudov, M.G.: Validation of reducing-difference procedure for the interpretation of non-polarized infrared spectra of *n*-component solid mixtures. *Talanta* **69**, 822–828 (2006)
- Ivanova, B.B., Simeonov, V.D., Arnaudov, M.G., Tsalev, D.L.: Linear-dichroic infrared spectroscopy—validation and experimental design of the orientation technique as suspension in nematic liquid crystal. *Spectrochim. Acta* **67A**, 66–75 (2006)
- Koleva, B.B., Kolev, T.M., Simeonov, V., Spassov, T., Spitteller, M.: Linear polarized IR-spectroscopy of partial oriented solids as a colloidal suspension in nematic liquid crystal—new tool for structural elucidation of the chemical compounds. *J. Incl. Phenomen.* **61**, 319–333 (2008). doi:10.1007/s10847-008-9425-5
- Ivanova, B.B.: Stereo-structural and IR-spectral characterization of histidine containing dipeptides by means of solid state IR-LD spectroscopy and ab initio calculations. *J. Mol. Struct.* **782**, 122–129 (2006)
- Ivanova, B.B.: IR-LD spectroscopic characterization of L-Tryptophan containing dipeptides. *Spectrochim. Acta* **64A**, 931–938 (2006)
- Ivanova, B.B., Kolev, T., Zareva, S.: Solid-state IR-LD spectroscopic and theoretical analysis of glycine-containing peptides and their hydrochlorides. *Biopolymers* **82**, 587–596 (2006)
- Kolev, T.s.: Solid-state IR-LD spectroscopic and theoretical analysis of arginine-containing peptides. *Biopolymers* **83**, 39–45 (2006)
- Jordanov, B., Schrader, B.J.: Reduced IR-LD spectra of substances oriented as nematic solutions. *J. Mol. Struct.* **347**, 389–398 (1995)
- Jordanov, B., Nentchovska, R., Schrader, B.: FT-IR linear dichroic solute spectra of nematic solutions as a tool for IR band assignment. *J. Mol. Struct.* **297**, 401–406 (1993)
- Michl, J., Thulstrup, E.W.: Spectroscopy with Polarized Light. Solute alignment by photoselection, in liquid crystals, polymers, and membranes. VCH Publishers, NY (1986)

24. Thulstrup, E.W., Eggers, J.H.: Moment directions of the electronic transitions of fluoranthene. *Chem. Phys. Lett.* **1**, 690–692 (1996)
25. Frisch, M.J., Trucks, G.W., Schlegel, H.B., Scuseria, G.E., Robb, M.A., Cheeseman, J.R., Zakrzewski, V.G., Montgomery, J.A. Jr., Stratmann, R.E., Burant, J.C., Dapprich, S., Millam, J.M., Daniels, A.D., Kudin, K.N., Strain, M.C., Farkas, Ö., Tomasi, J., Barone, V., Cossi, M., Cammi, R., Mennucci, B., Pomelli, C., Adamo, C., Clifford, S., Ochterski, J., Petersson, G.A., Ayala, P.Y., Cui, Q., Morokuma, K., Salvador, P., Dannenberg, J.J., Malick, D.K., Rabuck, A.D., Raghavachari, K., Foresman, J.B., Cioslowski, J., Ortiz, J.V., Baboul, A.G., Stefanov, B.B., Liu, G., Liashenko, A., Piskorz, P., Komáromi, I., Gomperts, R., Martin, R.L., Fox, D.J., Keith, T., Al-Laham, M.A., Peng, C.Y., Nanayakkara, A., Challacombe, M., Gill, P.M.W., Johnson, B., Chen, W., Wong, M.W., Andres, J.L., Gonzalez, C., Head-Gordon, M., Replogle, E.S., Pople, J.A.: *Gaussian 98*, Gaussian, Inc., Pittsburgh, PA (1998)
26. “DALTON”, a molecular electronic structure program, Release 2.0 (2005), <http://www.kjemi.uio.no/software/dalton/dalton.html>
27. Zhurko, G.A., Zhurko, D.A.: ChemCraft: tool for treatment of chemical data, Lite version build 08 (2005)
28. Tomasi, J., Persico, M.: Molecular interactions in solution: an overview of methods based on continuous distributions of the solvent. *Chem. Rev.* **94**, 2027–2094 (1994)
29. Barone, V., Cossi, M., Tomasi, J.: A new definition of cavities for the computation of solvation free energies by the polarizable continuum model. *J. Chem. Phys.* **107**, 3210–3213 (1997)
30. Cammi, R., Rossi, M., Benucci, B., Tomasi, J.: Analytical Hartree–Fock calculation of the dynamical polarizabilities α , β , and γ of molecules in solution. *J. Chem. Phys.* **105**, 10556–10559 (1996)
31. Kolev, T., Kityk, I., Ebothe, J., Sahraoui, B.: Intrinsic hyperpolarizability of 3-dicyanomethylene-5,5-dimethyl-1-[2-(4-hydroxyphenyl)ethenyl]-cyclohexene nanocrystallites incorporated into the photopolymer matrices. *Chem. Phys. Lett.* **443**, 309–312 (2007)
32. Ju, X., Ju, H., Zhao, H., Tao, X., Bian, W., Jiang, M.: Study of electronic and spectroscopic properties on a newly synthesized red fluorescent material. *J. Chem. Phys.* **124**, 174711–174716 (2006)